Supplement of Atmos. Chem. Phys., 22, 8497–8527, 2022
https://doi.org/10.5194/acp-22-8497-2022-supplement

Atmospheric Chemistry and Physics
Open Access
EGU

Supplement of

Investigation of the limonene photooxidation by OH at different NO concentrations in the atmospheric simulation chamber SAPHIR (Simulation of Atmospheric PHotochemistry In a large Reaction Chamber)

Jacky Yat Sing Pang et al.

Correspondence to: Hendrik Fuchs (h.fuchs@fz-juelich.de)

1. Nitrate wall loss rate

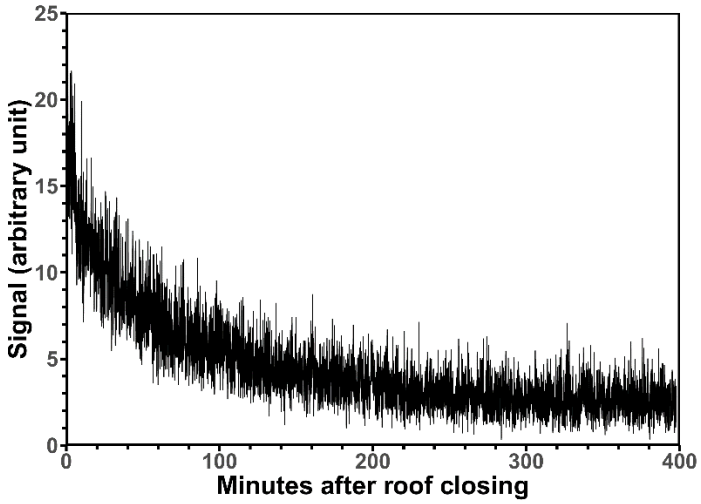

Figure S1. Nitrate ion CIMS signal for the compounds $C_{10}H_{17}NO_6$ (m/z 310) during a high NO (10 ppbv) limonene oxidation experiment (Zhao et al., 2018). The rate constant of this loss process is 8.46 $\times 10^{-3}$ min^{-1}.

2. Calculation of product yield

To calculate the time series of the product yield, chamber source and chemical loss processes have to be considered to correct the measured formaldehyde (HCHO) and limonene concentration (Rolletter et al., 2019). Both species are subject to dilution loss as a result of replenishing flow, this can be expressed as:

$$\Delta[x] = -k_{\mathrm{dil}}[x]\Delta t \quad \text{(S1)}$$

where [x] is the concentration of the chemical species; k_{dil} is the dilution constant measured during the experiment. HCHO has additional losses from photolysis and the reaction with OH. The calculation of these chemical loss processes ($\Delta[\mathrm{HCHO}]_{\mathrm{chem}}$) follows the description in the Master Chemical Mechanism version 3.3.1 (MCM v.3.3.1):

$$\Delta[\mathrm{HCHO}]_{\mathrm{chem}} = -(j_{\mathrm{HCHO}} + 5.4 \times 10^{-12} \exp\left(\frac{135}{T}\right)[\mathrm{OH}])[\mathrm{HCHO}]\Delta t \quad \text{(S2)}$$

where j_{HCHO} is the photolysis rate of HCHO. The corrected concentration is then iteratively calculated by using Eq. S1 and Eq. S2:

$$[\mathrm{LIM}]_{\mathrm{corr}_{t+1}} = [\mathrm{LIM}]_t + k_{dil_t}[\mathrm{LIM}]_t\Delta t \quad \text{(S3)}$$

$$[\mathrm{HCHO}]_{\mathrm{corr}_{t+1}} = [\mathrm{HCHO}]_t + (k_{dil_t} + J_{\mathrm{HCHO}_t} + 5.4 \times 10^{-12} \exp\left(\frac{135}{T}\right)[\mathrm{OH}]_t)[\mathrm{HCHO}]_t\Delta t \quad \text{(S4)}$$

$$[\mathrm{HCHO}]_{\mathrm{LIM_{oxd}}} = [\mathrm{HCHO}]_{\mathrm{corr}_{t+1}} - Q_{\mathrm{HCHO}} \quad \text{(S5)}$$

where $[LIM]_{corr}$ and $[HCHO]_{corr}$ are the corrected limonene and HCHO concentration respectively. To determine the amount of HCHO emitted from the chamber wall during the experiment, the chamber roof is opened to allow the chamber to be irradiated before limonene is injected into the chamber (zero-air phase). The production rate of chamber HCHO is then determined using the HCHO measurement during the zero-air phase. With this production rate, a control simulation in which no limonene is injected into the chamber is conducted, the resulting HCHO concentration is corrected using equation S4 to yield the HCHO concentration attributed from chamber source (Q_{HCHO}). The amount of HCHO produced from the oxidation of limonene ($[HCHO]_{LIMoxd}$) could be calculated by subtracting the corrected chamber-emitted HCHO concentration from Q_{HCHO}. To calculate the amount of reacted limonene, the following equation is followed:

$$\mathrm{LIM}_{\mathrm{reacted}_{t'}} = \sum_{t=0}^{t=t'}([\mathrm{LIM}] \times (k_{\mathrm{LIM+O_3}} \times [\mathrm{O_3}] + k_{\mathrm{LIM+OH}} \times [\mathrm{OH}])) \quad \text{(S6)}$$

where $LIM_{reacted\_t'}$ is the total amount of reacted limonene at time t', $[O_3]$ and [OH] are the measured O_3 and OH concentrations respectively.

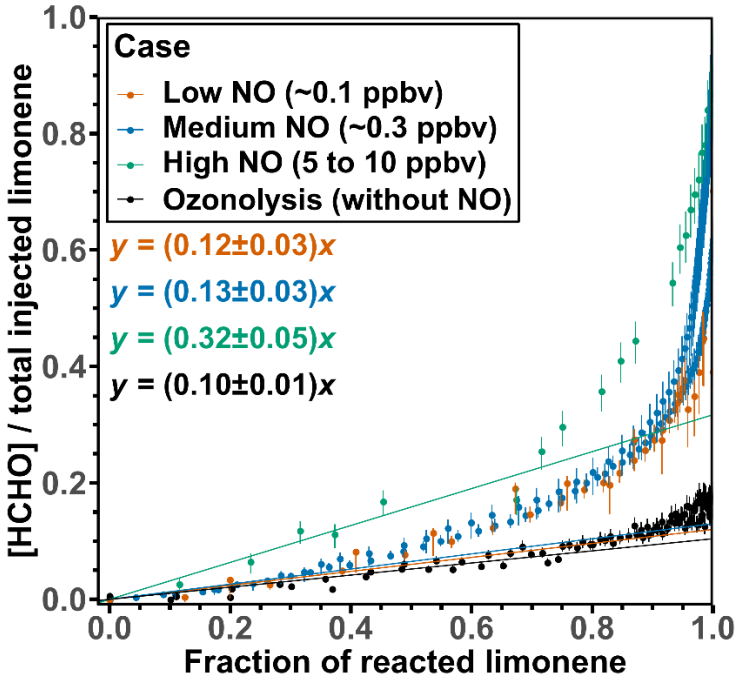

Figure S2. HCHO concentrations divided by the injected limonene concentration plotted versus the fraction of reacted limonene for the first injection in the experiments with different NO levels.

3. Model-measurement comparison for the other limonene oxidation experiments (Section 3.2 in the main text)

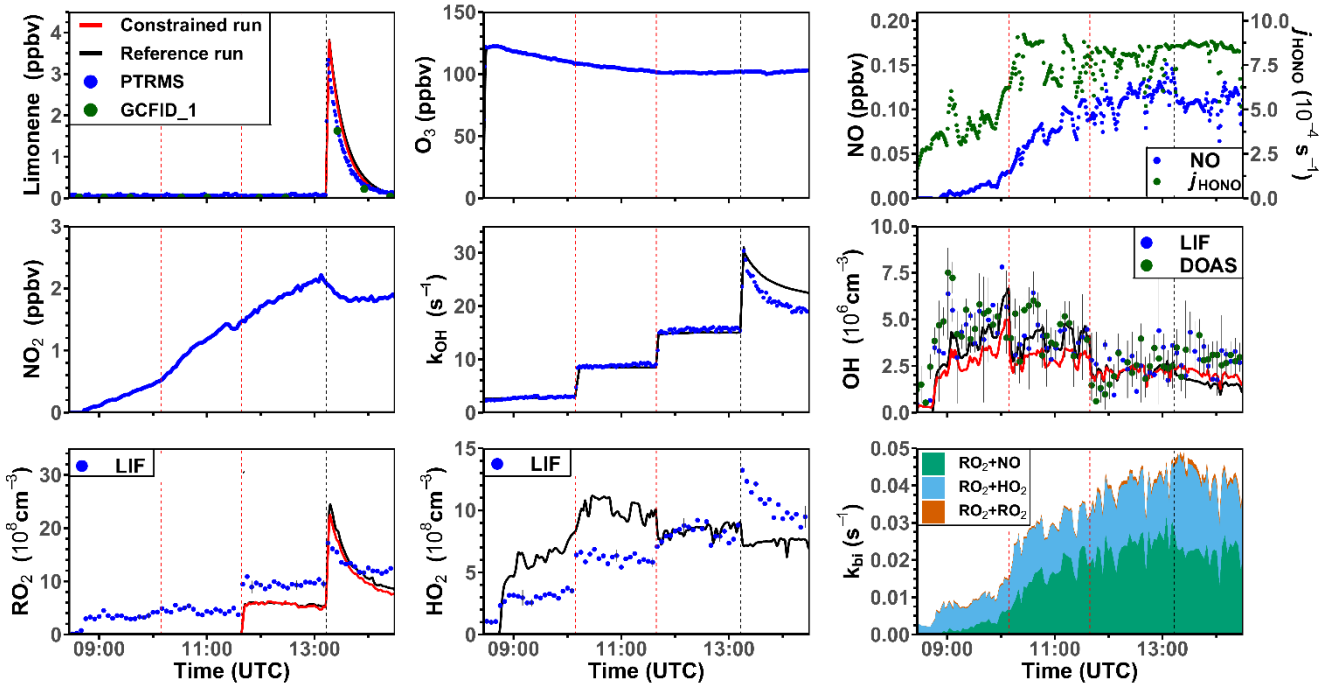

Figure S3. Time series of radicals, inorganic and organic species during the limonene oxidation experiment at low NO mixing ratio on 13 June 2015. The black line denoted the modelled results from the reference model with O_3, NO_x and HONO are constrained; the red line denoted the modelled results from the constrained model with HO_2 constrained and k_{OH} adjusted to the measurement, and the dots are the measurements. RO_2 bi-molecular reaction loss rate constant (k_{bi}) are calculated based on the measured NO, HO_2, and RO_2 concentrations using reaction rate constants from the MCM model. The first red dashed line indicates the injection of 750 ppb of CO; the second red dashed line indicates the injection of 60 ppm of CH_4.

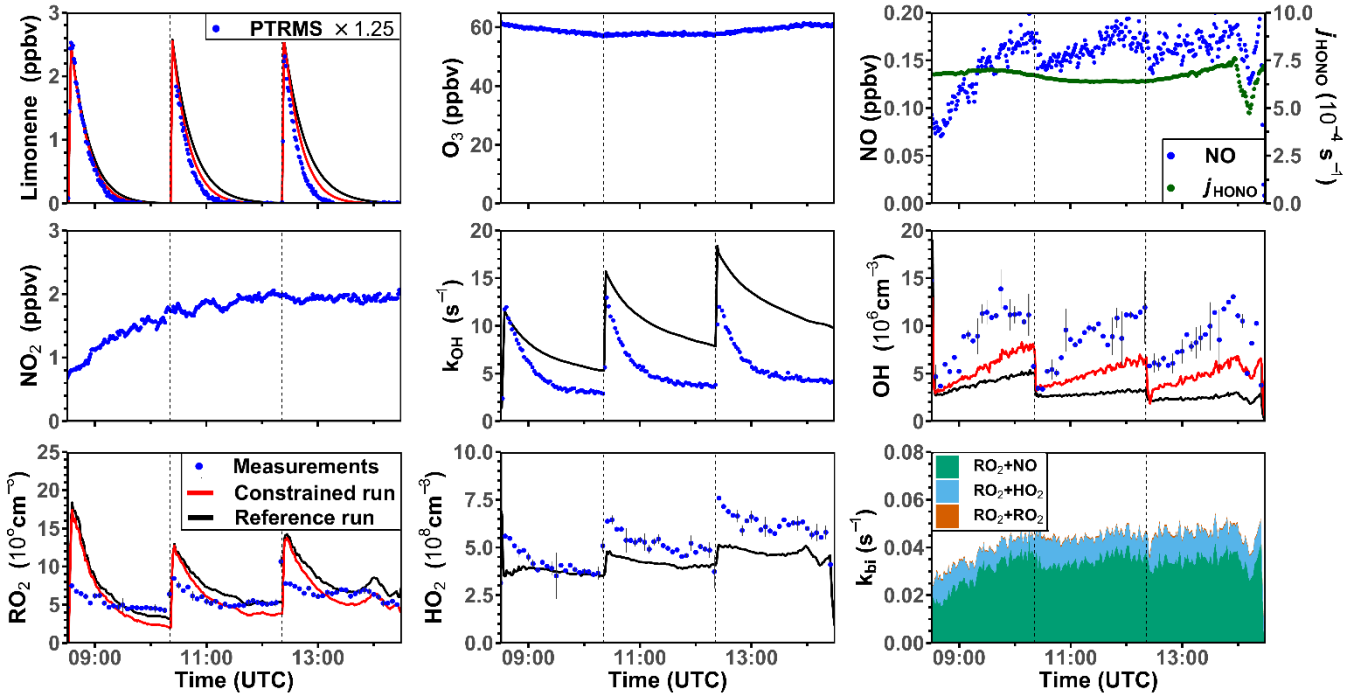

Figure S4. Time series of radicals, inorganic and organic species during the limonene oxidation experiment at low NO mixing ratio on 04 July 2019. Limonene concentrations measured by PTRMS are scaled by a factor of 1.25 to match the increase of OH reactivity during limonene injections. The black line denoted the modelled results from the reference model with O_3, NO_x and HONO being constrained; the red line denoted the modelled resulted from the constrained model with HO_2 constrained and k_{OH} adjusted to the measurement. RO_2 bi-molecular reaction loss rate constant (k_{bi}) are calculated based on the measured NO, HO_2, and RO_2 concentrations using reaction rate constants from the MCM model.

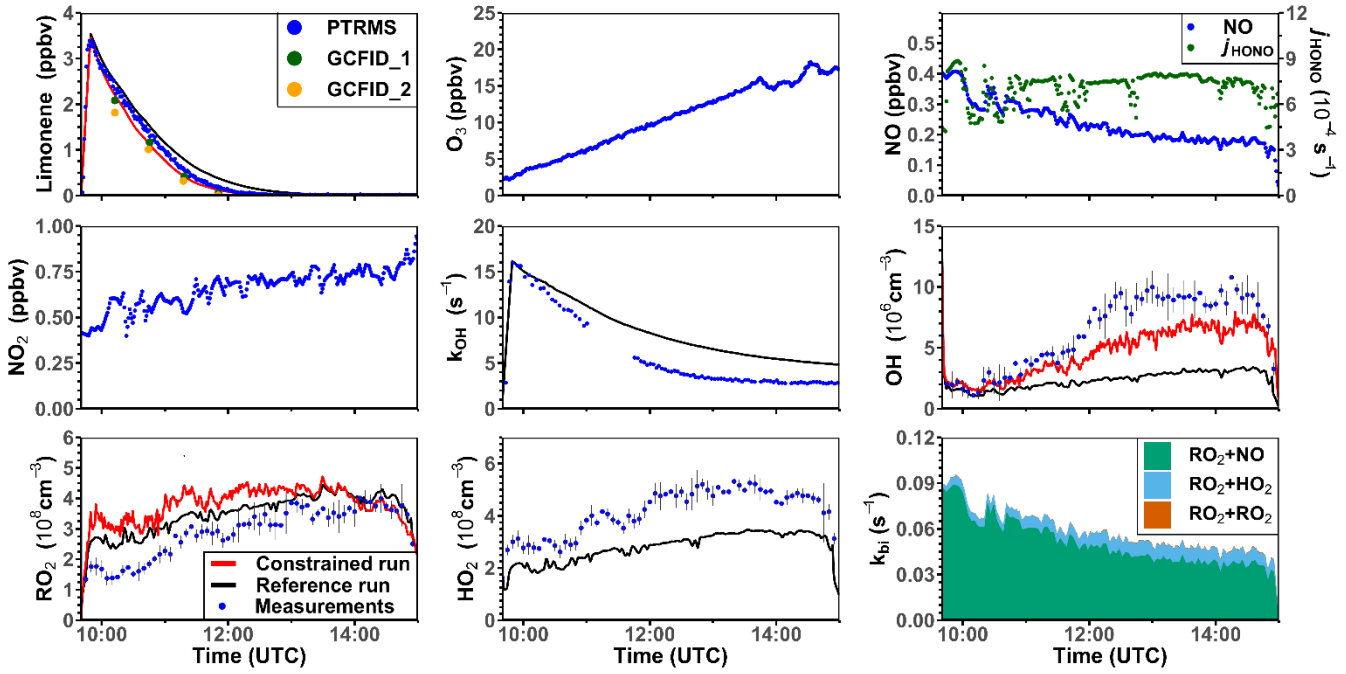

Figure S5. Time series of radicals, inorganic and organic species during the limonene oxidation experiment at medium NO mixing ratio on 10 August 2012. The black line denoted the modelled results from the reference model with O_3, NO_x and HONO being constrained; the red line denoted the modelled resulted from the constrained model with HO_2 constrained and k_{OH} adjusted to the measurement. RO_2 bi-molecular reaction loss rate constant (k_{bi}) are calculated based on the measured NO, HO_2, and RO_2 concentrations using reaction rate constants from the MCM model.

4. Contribution of k_{OH} from limonene oxidation products and intermediates

OH reactivity is overestimated at all limonene oxidation experiments after limonene injections. To identify the contribution to the total k_{OH} from limonene oxidation products and intermediates, the total k_{OH} is subtracted by the k_{OH} attributed to limonene and the background with the following formula:

$$k_{\mathrm{OH_{intermediates}}} = k_{\mathrm{OH_{total}}} - 4.28 \times 10^{-11} \times \exp\left(\frac{401}{T}\right) \times [\mathrm{LIM}] - k_{\mathrm{OH_{background}}}$$

where $k_{OH_{total}}$ is the total measured or simulated OH reactivity; [LIM] is the limonene concentration; $k_{OHbackground}$ is the OH reactivity contributed by unknown contaminants (k_{OH} ~ 1 s^{-1}) and inorganic compounds (e.g., NO, O_3). Contribution to $k_{OH_{intermediates}}$ from different groups of species is also calculated, which includes acyl peroxy nitrates (PANs), organic nitrates ($RONO_2$), organic peroxide (ROOH), first-generation product of limonene ozonolysis (O_3 1st gen.), first-, second-, and third-

generation products from limonene-OH oxidation (OH 1st gen., OH 2nd gen., and OH 3rd gen.) (Table S1). Reaction rate constants of limonene and its intermediates with OH and O_3 are all taken from the MCM.

Group	MCM species
OH 1st gen.	LIMAL, LIMKET
OH 2nd gen.	LMLKET
OH 3rd gen.	CO25C6CHO, C517CHO, HMVKBCHO
O_3 1st gen.	C622CHO, C624CHO, C729CHO
ROOH	LIMAOOH, LIMBOOH, LIMCOOH, LMKAOOH, LMKBOOH, LIMALOOH, C817OOH, C926OOH, LIMALAOOH, LIMALBOOH, C923OOH, C924OOH, C728OOH, C622OOH, C826OOH, C729OOH, C627OOH, C818OOH, C517OOH
RONO2	LIMANO3, LIMBNO3, LIMCNO3, LMKANO3, LMKBNO3, LIMALNO3, C923NO3, C817NO3, C728NO3, C826NO3, C517NO3
PANs	C923PAN, C822PAN, C729PAN, C622PAN, C817PAN, C626PAN, C823PAN, C727PAN, C627PAN, C517PAN, C5PAN2, HMVKBPAN, PHAN, PAN

Table S1. MCM species that are included for the calculation of the contribution to $k_{OH\_intermediate.}$

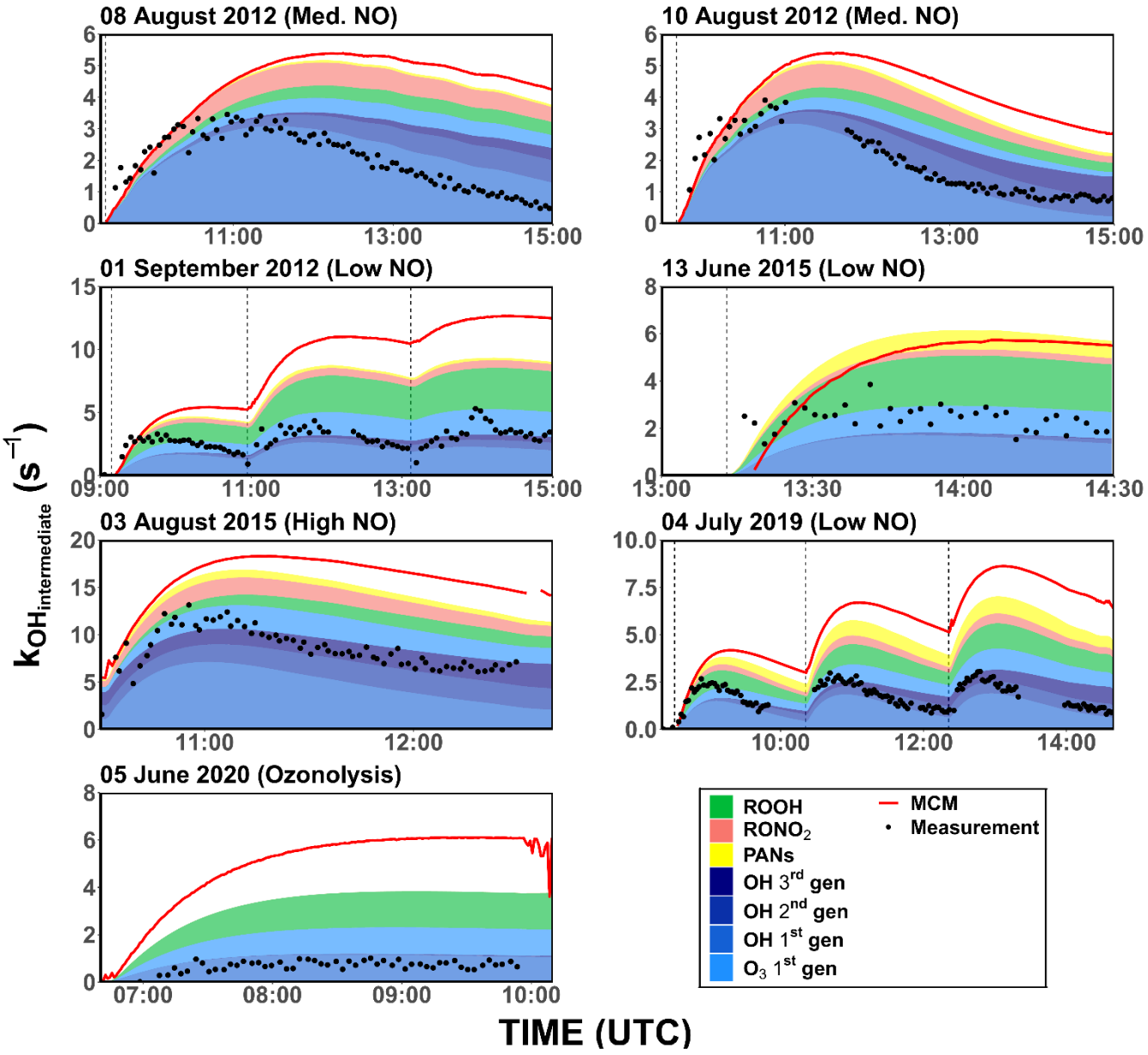

110 **Figure. S6** OH reactivity (k_{OH}) contributions from the oxidation of limonene-derived products and intermediates from the measurements and modelled values. The model results are based on the constrained model run (O_3, NO_x, HONO, and HO_2 are constrained). The modelled total OH reactivity, $k_{OH_{intermediate}}$, is less than sum of single contributions on 13 June 2015, because the slowly increasing chamber background reactivity is not captured throughout the experiment.

5. Experimental OH radical budget for other experiments (Section 3.3 in the main text)

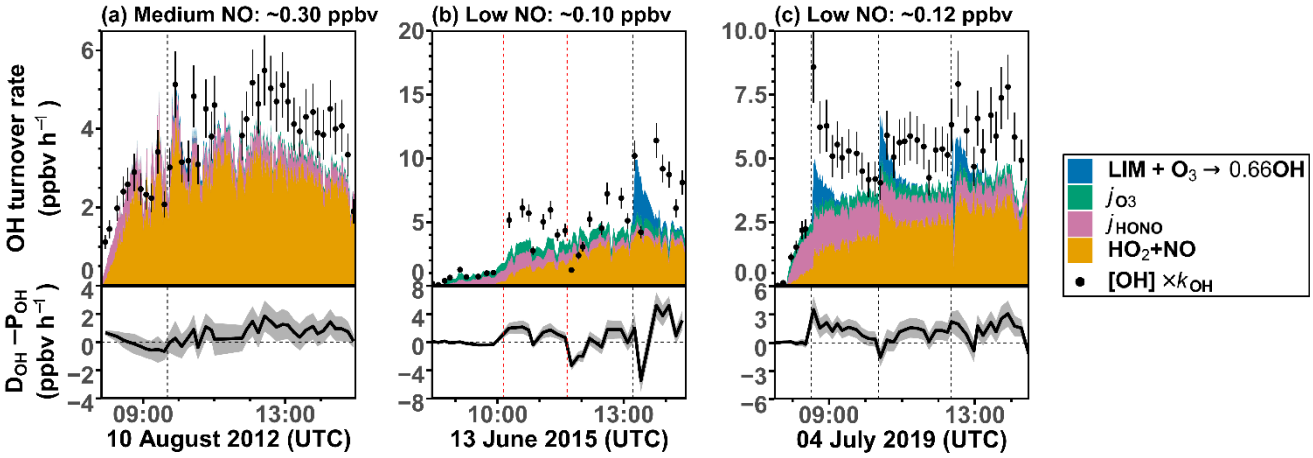

Figure S7. Simliar to Fig. 8 in the main text. 10-minutes-average values of total OH destruction rates compared to the sum of OH production rates from the main OH sources that can be calculated from measurements. Shaded areas in the difference plots give the uncertainties of the calculations. Production of OH from the reaction of O_3 and HO_2 was negligible (< 0.01 ppbv h^{-1}) for conditions of the experiments.

6. Composition of RO_2 in the simulation (Section 3.4 in the main text)

To identify the cause of the overestimation of peroxy radicals in the low NO_x and the ozonolysis experiments, concentrations of the peroxy radicals from the oxidation reaction are calculated and divided into four groups. The first group consists of the three peroxy radicals from the oxidation of limonene by OH, which includes LIMAO2, LIMBO2 and LIMCO2 (naming follows the MCM); the second group consists of the main peroxy radicals that are produced from limonene ozonolysis, which includes LIMALAO2, LIMALBO2, and CH3CO3; the third group consists of C923O2 and C924O2, which is the minor peroxy radical products from the ozonolysis reaction and one of the peroxy radicals produced from the OH-oxidation of the first-generation OH-oxidation product; and the fourth group is the methyl peroxy radical (CH_3O_2), which is produced from reactions of CH3CO3 as well as the oxidation of methane during the experiment on 13 June 2015.

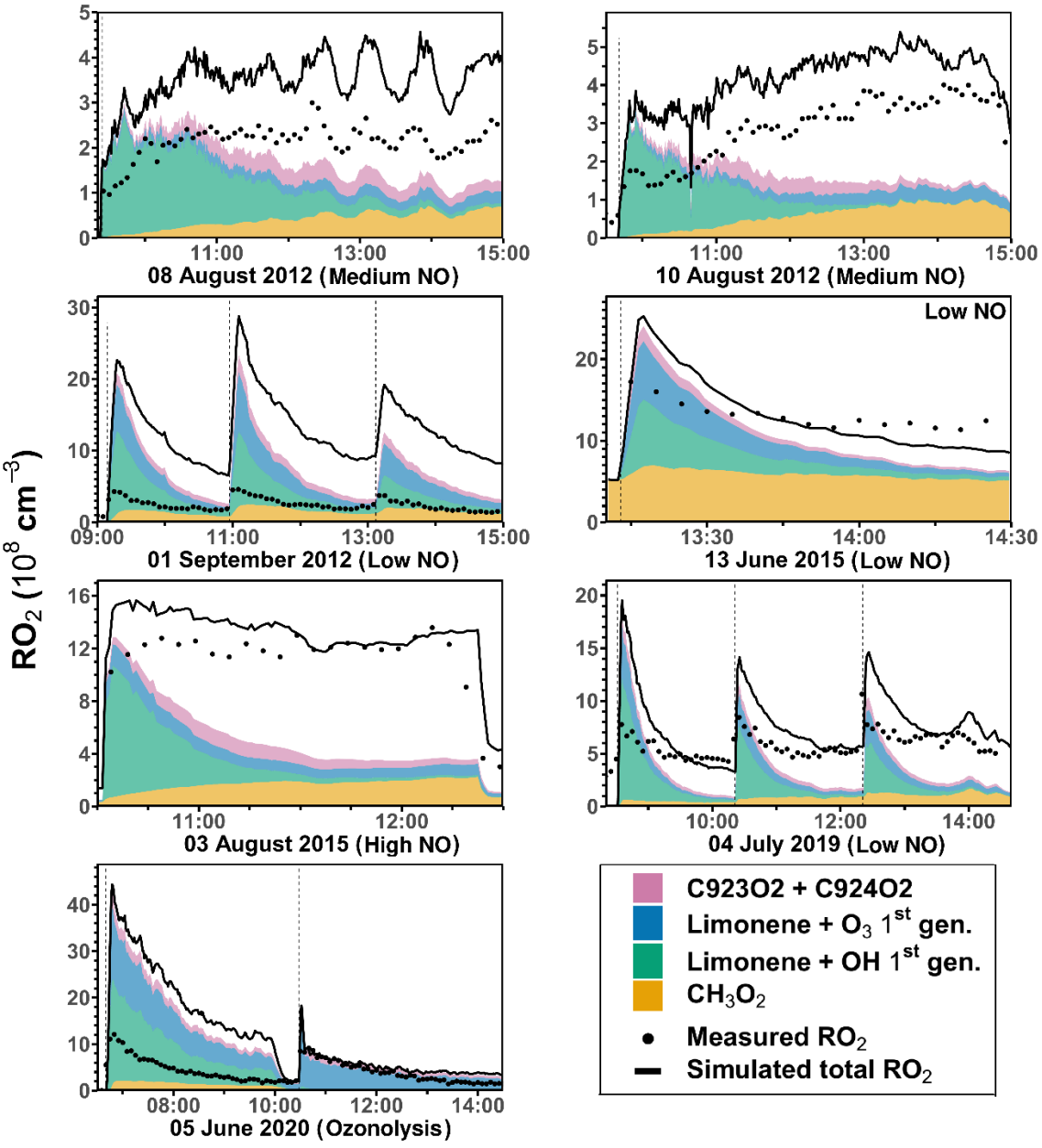

Figure S8. Similar to Fig. 9 in the main text. The total RO_2 radical concentrations and their speciation from model calculations (constrained model run) compared to the measured values for all the experiments. Methylperoxy radicals (CH_3O_2) are mainly produced from the oxidation of HCHO in most of the experiments or from the oxidation of CH_4 during the experiment on 13 June 2015. Radicals directly produced from the reaction of limonene with either OH or O_3 are summed. C923O2 + C924O2

are RO_2 radicals produced from the further oxidation of the first-generation oxidation products. Names are taken from the MCM.

7. Impacts of RO_2 model results on the modelled NO_x concentrations (Section 3.5 in the main text)

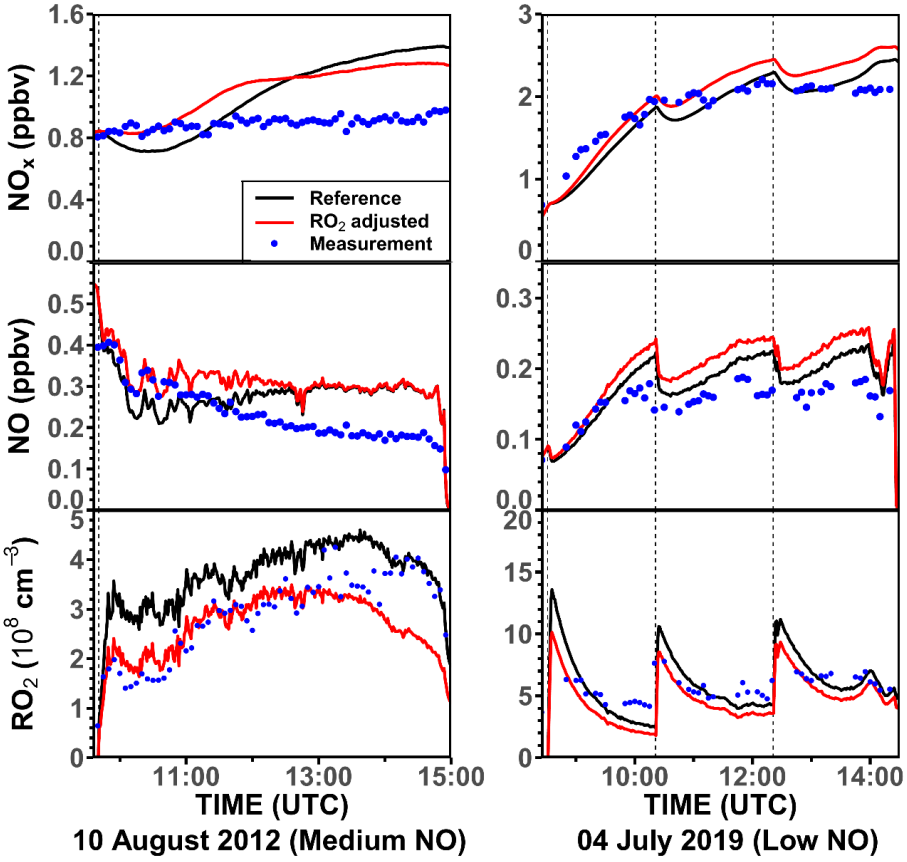

Figure S9. Similiar to Fig. 10 in the main text. Example of the impact of modelled RO_2 on the modelled NO_x and NO concentrations in the experiments with medium NO (10 August 2012) and low NO (04 July 2019) concentrations. In both cases, the organic nitrate yield for the first-generation RO_2 from the limonene+OH reaction is taken from the analysis in this work (34%).

8. Sensitivity run (Section 4.1 in the main text)

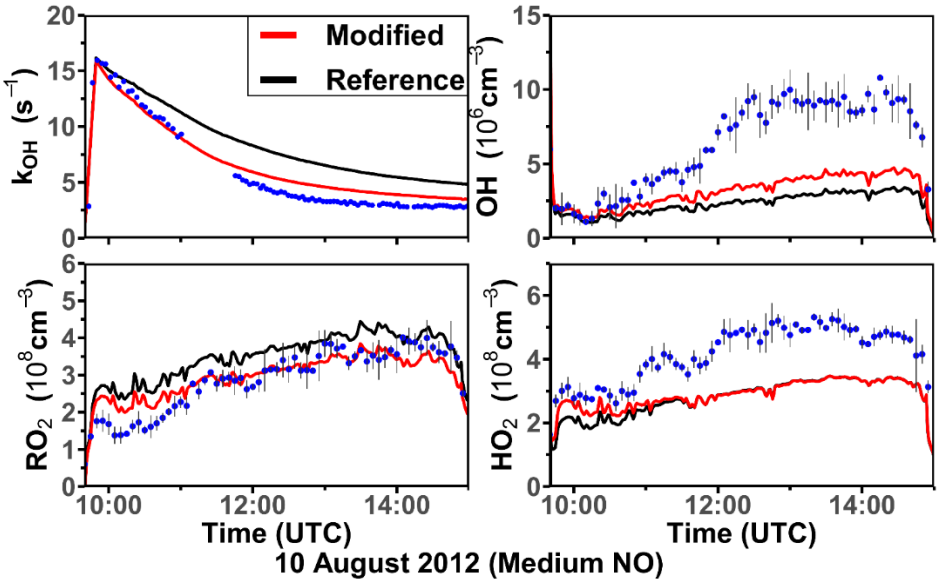

Figure S10. Similar to Fig. 12 to Fig. 14 in the main text. Modelled and measured OH reactivity, HO_2, RO_2, and OH concentrations for the experiments with medium NO concentrations on 10 August 2012. Results from the reference model (reference) and the sensitivity model run (modified) that includes additional RO_2 loss processes that produce HO_2.

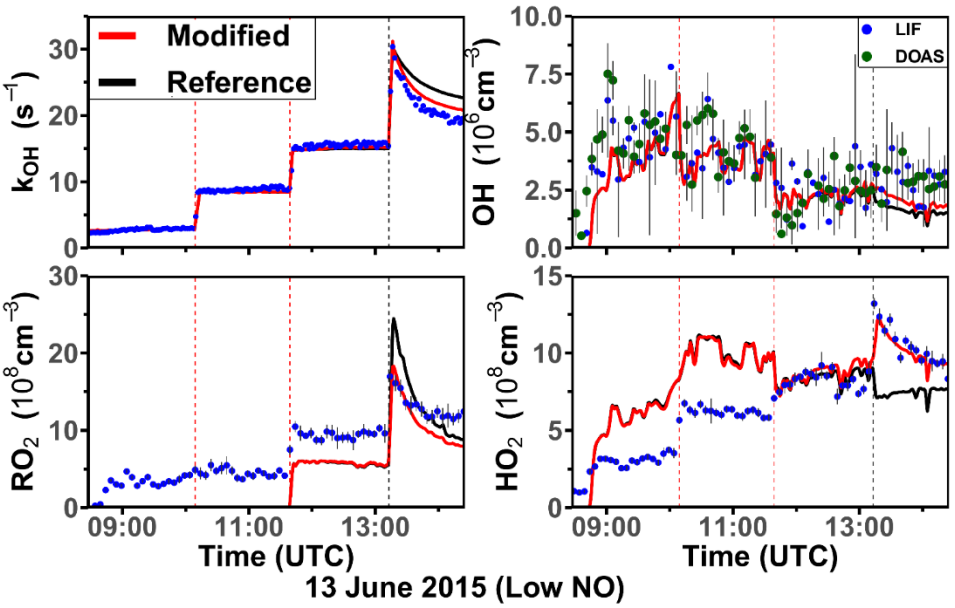

Figure S11. Similar to Fig. 12 to Fig. 14 in the main text. Modelled and measured OH reactivity, HO_2, RO_2, and OH concentrations for the experiments with low NO concentrations on 13 June 2015. Results from the reference model (reference) and the sensitivity model run (modified) that includes additional RO_2 loss processes that produce HO_2.

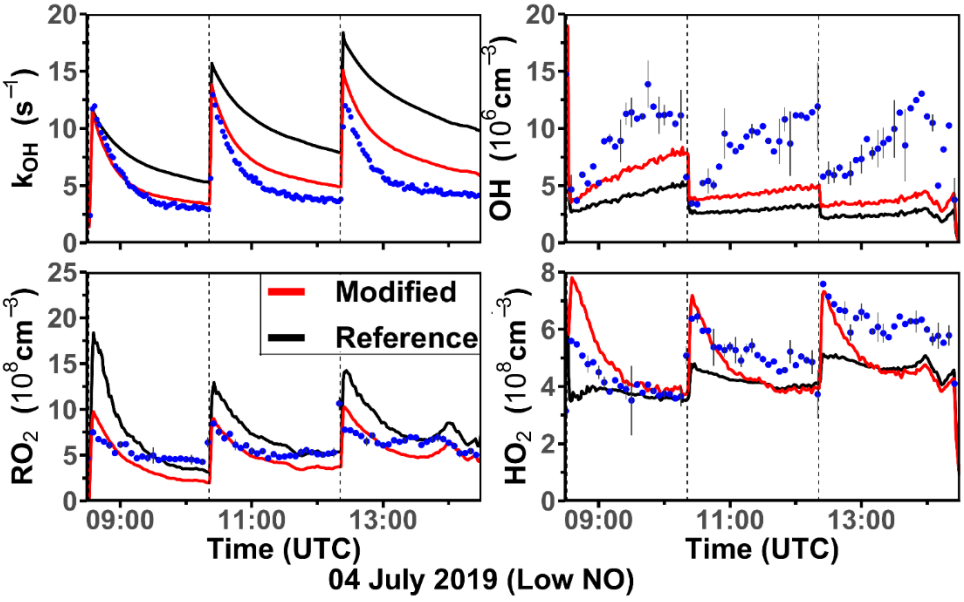

Figure S12. Similar to Fig. 12 to Fig. 14 in the main text. Modelled and measured OH reactivity, HO_2, RO_2, and OH concentrations for the experiments with low NO concentrations on 04 July 2019. Results from the reference model (reference) and the sensitivity model run (modified) that includes additional RO_2 loss processes that produce HO_2.

Reference

Rolletter, M., Kaminski, M., Acir, I.-H., Bohn, B., Dorn, H.-P., Li, X., Lutz, A., Nehr, S., Rohrer, F., Tillmann, R., Wegener, R., Hofzumahaus, A., Kiendler-Scharr, A., Wahner, A., and Fuchs, H.: Investigation of the α-pinene photooxidation by OH in the atmospheric simulation chamber SAPHIR, Atmos. Chem. Phys., 19, 11635–11649, https://doi.org/10.5194/acp-19-11635-2019, 2019.

Zhao, D., Schmitt, S. H., Wang, M., Acir, I.-H., Tillmann, R., Tan, Z., Novelli, A., Fuchs, H., Pullinen, I., Wegener, R., Rohrer, F., Wildt, J., Kiendler-Scharr, A., Wahner, A., and Mentel, T. F.: Effects of NO_x and SO_2 on the secondary organic aerosol formation from photooxidation of α-pinene and limonene, Atmos. Chem. Phys., 18, 1611–1628, https://doi.org/10.5194/acp-18-1611-2018, 2018.